Topology Optimization of Structural Continuous Yarn Polymer Composites

O. Abdul-Ghani, N. Laflamme, R. Hébert and F. Robitaille*

Department of Mechanical Engineering, University of Ottawa, Ottawa ON, Canada

* *Corresponding author (francois.robitaille@uottawa.ca)*

Keywords: *topology optimization; continuous yarns; design; manufacturing*

1. Abstract

This paper presents a design methodology for structural PMC parts reinforced by continuous yarns and featuring 3D topology optimization. The method was developed for manufacturability: PMC parts start as triangulated structures of tensioned yarn arrays extending in 3D, wrapped around fixed guide surfaces and interlaced within the part envelope. Resin is consolidated and cured at a later stage, creating PMC parts with atypical geometries differing from classic beams, tubes or shells. The paper describes part design and manufacturing design up to final yarn paths in the parts. The vector field of principal stresses is obtained from finite element analysis of continuous isotropic material within the part envelope. Select stress paths are defined from chosen seed points and used as basis for *k*-neighbours triangulation of the optimized part. Yarn paths are then derived.

2. Introduction

Polymer-matrix composites (PMCs) reinforced with continuous yarns are ideal for dynamic structural applications because of their exceptional specific mechanical properties. However, recent decades have seen the parallel emergence of additive manufacturing (AM) processes for metal alloy parts. AM makes topological optimization (TO) of metal parts possible, with metal deposited only along high stress paths for any given load case. AM and TO enable metal parts that are highly efficient on a mass basis, competing with PMCs over one of their main advantages [1].

PMC manufacturing is inherently additive. However, true TO has not happened yet for PMC parts, for two reasons [2]. Firstly, continuous yarns in structural PMCs must align with directions of high stress in 3D, making manufacturing difficult. Reported parts are either semi-structural and feature short fibres, or they feature continuous yarns [3–5] extending in 2D layers only for simpler cases where this can lead to an optimal solution [6]. Secondly, PMC manufacturing generally makes beams and shells as opposed to irregular lattice parts. Reported truss-like PMC structures typically feature a repeating basic structural unit [6–12]; few examples of non-repeating 3D PMC lattices were reported [13]. As a result, AM metal parts can outperform PMC parts despite superior specific material properties for PMCs. This work addresses PMC 3DTO part and process design, with the aim of increasing the performance of PMC parts featuring continuous carbon yarns [14-16].

3. Literature

3.1. Topology optimization for PMCs and fibre orientation control

Analytical work aiming at applying TO to PMCs was proposed [3, 4]. Density-based approaches linking element density to elastic modulus [5] such as the solid isotropic material with penalization (SIMP) method are typically used as a starting point. Challenges arise as PMC properties depend not only on position but also on orientations of reinforcement yarns that are continuous: designing PMC parts involves more variables. Hence, modifications to SIMP were proposed to account for orthotropy by including fibre orientations inside each element [6].

TO applied to PMC parts is either sequential or concurrent. Sequential TO decouples the design processes, determining topology first and then optimizing fibre orientations [5]. Concurrent TO determines part topology and optimal fibre orientations simultaneously. Nomura [7] and Lee [8] succeeded with sequential TO applied to PMCs, optimizing topology and orientations at contained computational cost. Zhou [9], Setoodeh [10] and Xu [11] used alternative methodologies refining topology and fibre orientations iteratively. Recent progress with sequential TO aimed at increasing both performance and manufacturability. Yang [12] increased part stiffness by aligning continuous fibre orientations with principal stress directions obtained from FEA. Zhang [13] utilized streamline trajectories of principal stress vector fields for continuous fibre placement.

Concurrent TO has been sought-after in expectation of higher performance PMC parts [17, 18] despite higher complexity and cost [19-21]. Different authors [20, 23-25] proposed density-based methods featuring density and orientations as design variables. Stress lines tangent to optimized fibre orientations in each cell lead to increased stiffness and continuous yarn paths. However, most methods were tested on simpler cases of 2D geometries and applied loads, and may not generalize readily to realistic but more complex 3D geometries nor lead to straightforward manufacturing [22]. It is noted that Ye et al. [23] did use their framework on one 3D geometry, demonstrating capability in aligning fibres with local principal stress directions and achieving improved stiffness and an optimized final design with continuous yarns.

TO applied to PMCs has been addressed in approaches that are primarily computational. Reduced compliance and continuous fibre paths were obtained. However, the challenge of creating optimal fibre layouts for complex 3D geometries and making them physically manufacturable with continuous yarns extending along continuous trajectories largely remains.

3.2. Manufacturing of 3D printed PMC parts

Attempts at manufacturing PMC parts featuring continuous yarns through adaptations of 3D printing methods were presented, with the aim of improving specific structural properties of parts [26]. Issues identified relate mostly to manufacturing limitations in laying and directing continuous yarns over complex geometries featuring topology optimization. A few examples are discussed.

Adaptations and variations to Fused Deposition Modelling (FDM) were developed, with parameters probed including materials, yarn paths used in optimized parts, nozzle modifications and others. Early published work featuring 3D printing with continuous yarn PMCs [27-29] proposed one-step in-nozzle impregnation where a thermoplastic filament and continuous yarn were combined in a heated nozzle immediately before deposition of flat layers. Filaments were deposited as flat superimposed horizontal layers in a process similar to FDM using neat thermoplastic polymers. Results showed approximately fivefold increases in tensile modulus and tensile strength over neat polymers, demonstrating improvement over conventional short-fibre reinforced polylactic acid (PLA) polymer-based 3D printed parts but tellingly, still using these in comparisons. Both carbon fibres and jute fibres were featured as reinforcements.

Fracture imaging of specimens showed significant fibre pullout, with suboptimal impregnation and adhesion of polymer to fibres. Voids were present, and fibre volume fractions v_f in deposited PMCs remained at 40% to 50%. Results showed promise but continuous yarns were limited to flat superimposed planes with no topology optimization in 3D.

Additive Fiber Tethering (AFT) was proposed for manufacturing continuous yarn PMCs featuring topology optimization, inspired by truss-based lattices [30] and a technique called 3D coreless filament winding [31]. Coreless filament winding uses continuous yarns pre-impregnated with a thermosetting polymer in creating hollow interlaced designs featuring direct, yarn-to-yarn interactions rather than a traditional winding mandrel. The technology demonstrates the possibility of manufacturing topology optimized PMC parts where yarns interlace directly within a delimited 3D envelope, without other support, as envisaged in the present work.

AFT enables the manufacturing of PMC parts featuring complex geometry and 3D topology optimization by combining scaffolds and advanced filament winding. The process begins with an architected topology design based on face- and body-centered cubic lattice structures. A corresponding physical scaffold is designed, enabling the guiding of continuous yarns whilst ensuring their dimensional stability. Scaffolds are designed with strategically positioned anchor points enabling tethering of the yarns and ensuring transition between different yarn paths. Yarn path planning is based on a modified Hierholzer's algorithm, a graph-based approach designed for generating optimal Eulerian paths with reduced redundant yarn deployment, uninterrupted fibre placement and material waste. The paths are converted into machine-readable form and implemented in a robotic system; dry carbon yarns are impregnated in-situ with a thermosetting resin, the part is left to cure, and scaffolds and removed. Despite ongoing challenges, perhaps more specifically regarding manufacturing approach and methods, the work provides strong supportive evidence for further exploration of 3D topology optimization applied to structural PMC parts of complex geometry featuring continuous yarns.

3.3. Industrial efforts

A limited number of industrial efforts were devoted to proposing PMC parts featuring some of the characteristics mentioned above; these efforts met varied levels of adoption. Specific industrial actors are not mentioned here; rather, different approaches are briefly highlighted.

Traditional layered printing using continuous yarn filament is a commercial reality offered by a number of industrial actors; however, it does not enable TO in full 3D. Laying pre-impregnated yarns in 3D self-supported via fast curing resin is available; part geometries, thicknesses and yarn orientations are limited by the manufacturing method. Finally, infill or overlay reinforcement of polymer parts with directed yarns is relatively common; PMCs make up a fraction of part volume.

4. Design cases and initial FEA analysis

The part and process design method for 3DTO PMCs is sequential. In step 1, static linear elastic structural finite element analysis (FEA) is performed on isotropic material bound by the part envelope, for set loads and boundary conditions; commercial software ABAQUS was used. The principal stress vector field is extracted. Figure 1 shows two demonstrators, modified GE bracket subjected to upward forces on the left and centre, and simplified asymmetric torsion link subjected to tension on the right. Principal stress vector fields appear in Figure 2.

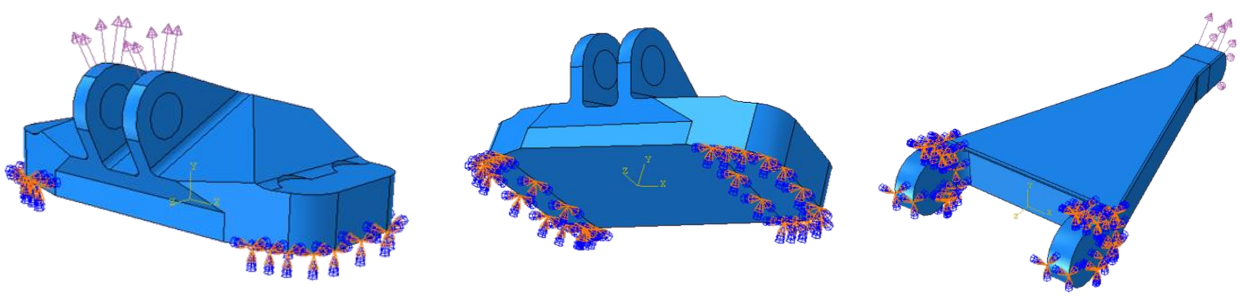

Figure 1. Demonstrator parts, loads and boundary conditions; modified GE bracket left and centre, simplified asymmetric torsion link right.

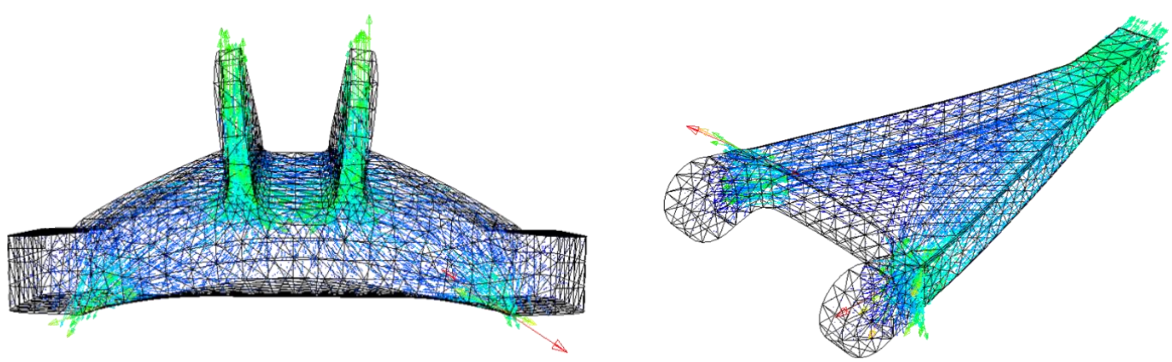

Figure 2. Principal stress vector fields; modified GE bracket left, simplified asymmetric torsion link right.

5. Stress path generation and selection

5.1. Seed point placement

Step 2 consists in creating seed points for stress paths. Step 2.1 illustrated left of Figure 3 ensures that seed points appear in all geometric features within the envelope. A uniform rectilinear grid of seed points with independent, feature-based spacing along x, y and z is created. Seed points located within the envelope are retained; each falls within an element but is not forced to its centroid. Step 2.2 illustrated right of Figure 3 ensures that seed points appear in high stress zones. Seed points are created at the centroid of the most loaded elements and filtered for relative distance, both operations defined by adjustable thresholds. Seed points are also created on edges of zones defining applied loads and boundary conditions as these must be present in final 3DTO PMC parts.

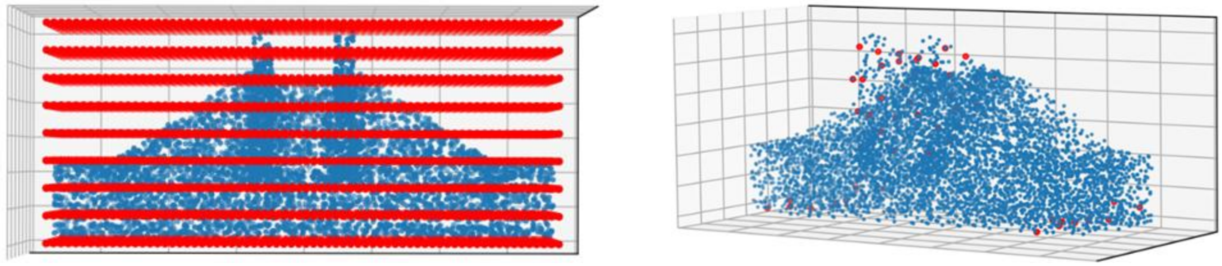

Figure 3. Seed points for modified GE bracket; rectilinear grid with feature-based spacing left, filtered points in high stress zones right

5.2. Stress path creation and selection

Step 3 consists in generating initial stress paths from seed points. Initial stress paths extend in both opposite directions from seed points, element to element, tangentially to local principal stress vectors until part envelope is reached or change in direction exceeds a set threshold. Initial stress paths appear in Figure 4 top left for modified GE bracket and centre for asymmetric torsion link. Seed points appear in green in the figure.

Step 4 consists in selecting stress paths towards generating the 3DTO part structure. In step 4.1 paths are prioritized based on an adjustable combination of path length and average stress level. In step 4.2 stress paths originating from seed points located at ends of edges defining zones of applied loads and boundary conditions segments building are added; some stress paths generated in steps 4.1 and 4.2 may be the same. Practical utilities were included to give the designer control beyond adjustable parameters: symmetric paths may be copied in symmetric parts, and nearly overlapping paths may displaced and/or merged. Selected stress paths also appear in Figure 4 for the same two demonstrators.

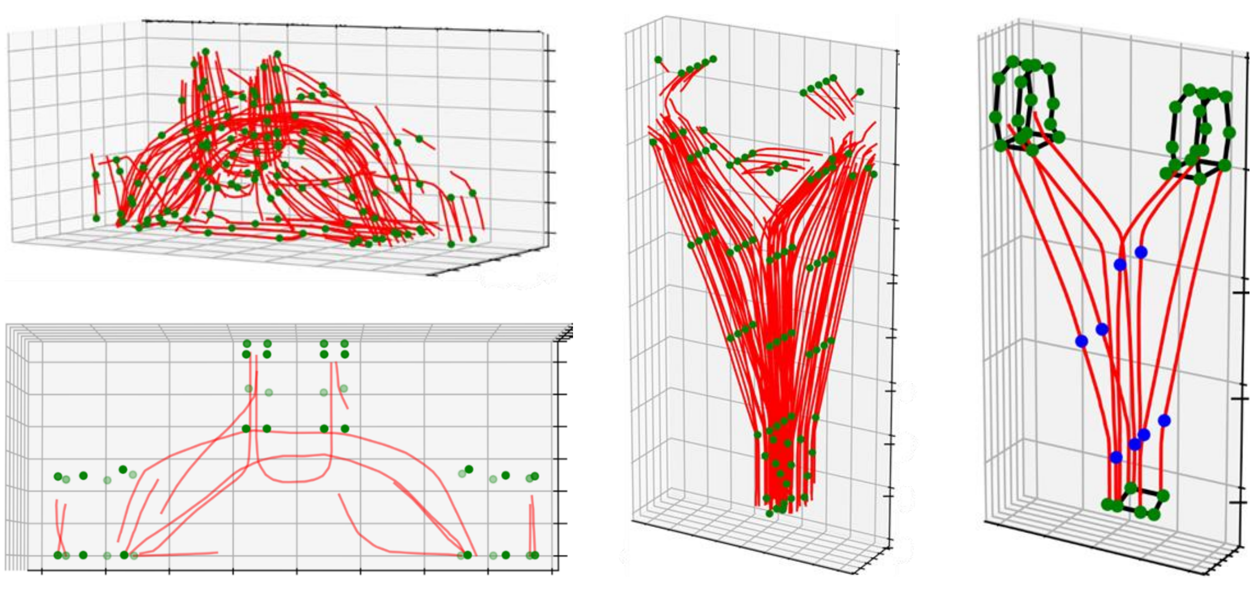

Figure 4. Initial and selected stress paths for modified GE bracket and simplified asymmetric torsion link.

6. Structure generation

Step 5 consists in creating a continuous structure from the selected stress paths using *k*-neighbours triangulation. Edges defining zones of applied loads and boundary conditions are added to the structure first. Then *n* points are sampled along each selected stress path. Finally, *k* straight edges are created for each point, extending from each fixed point and stress path point to their *k* closest neighbours. The resulting structure is defined by values of *k* and *n* chosen for manufacturability and structural performance; different values may be probed by the designer. Practical utilities were included to give the designer control beyond algorithmic triangulation: straight edges can be added or removed manually, facilitating reduction in edge clustering close to curved envelope boundaries where numerous points are defined, for example. Resulting structures appear in Figure 5.

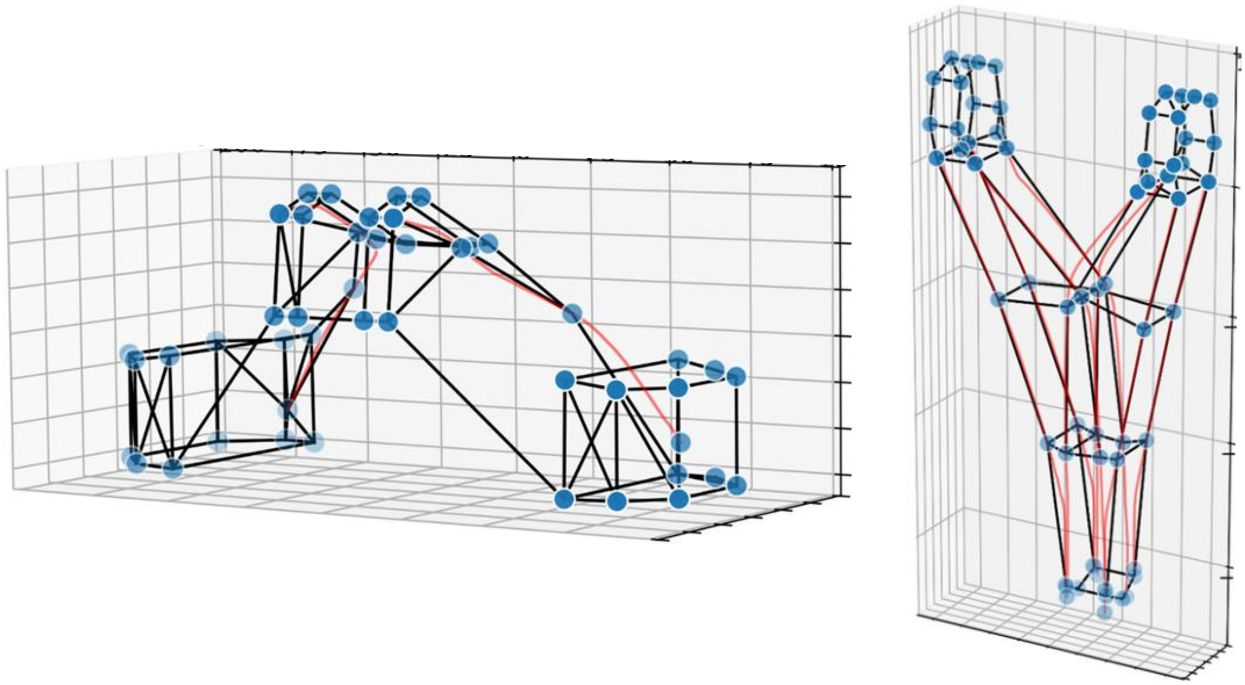

Figure 5. Triangulated structures generated for the modified GE bracket left, simplified asymmetric torsion link right.

7. Yarn path generation

Step 6 consists in defining the final paths along which groups of yarns will extends within the 3DTO PMC structure/part envelope, interlacing with a support structure and/or among themselves. Each yarn path follows a different sequence of edges. Collectively, yarns laid along these paths constitute the complete 3DTO reinforcement dry structure.

Two requirements guide yarn path generation using Dijkstra's algorithm. First, paths must originate and end on the part envelope, enabling adequate securing and tensioning of the yarns. All paths cross the envelope through the same two entry/exit points, facilitating manufacturing. Secondly, these entry/exit points are positioned at opposite ends along the longest dimension, promoting a smaller number of longer paths covering all the structure, further facilitating manufacturing. Different paths may overlap over any given edge in the final structure. However, edges reused upon generating a new path are penalized, reducing the number of such overlaps and balancing the number of paths, hence yarns, present along any given edge in the final structure.

Figure 6 shows five examples of yarn paths for the simplified asymmetric torsion link; the complete structure required 24 paths. The lower right part of the figure shows the numbers of yarn segments present over each edge. The figure shows that the numbers are generally contained.

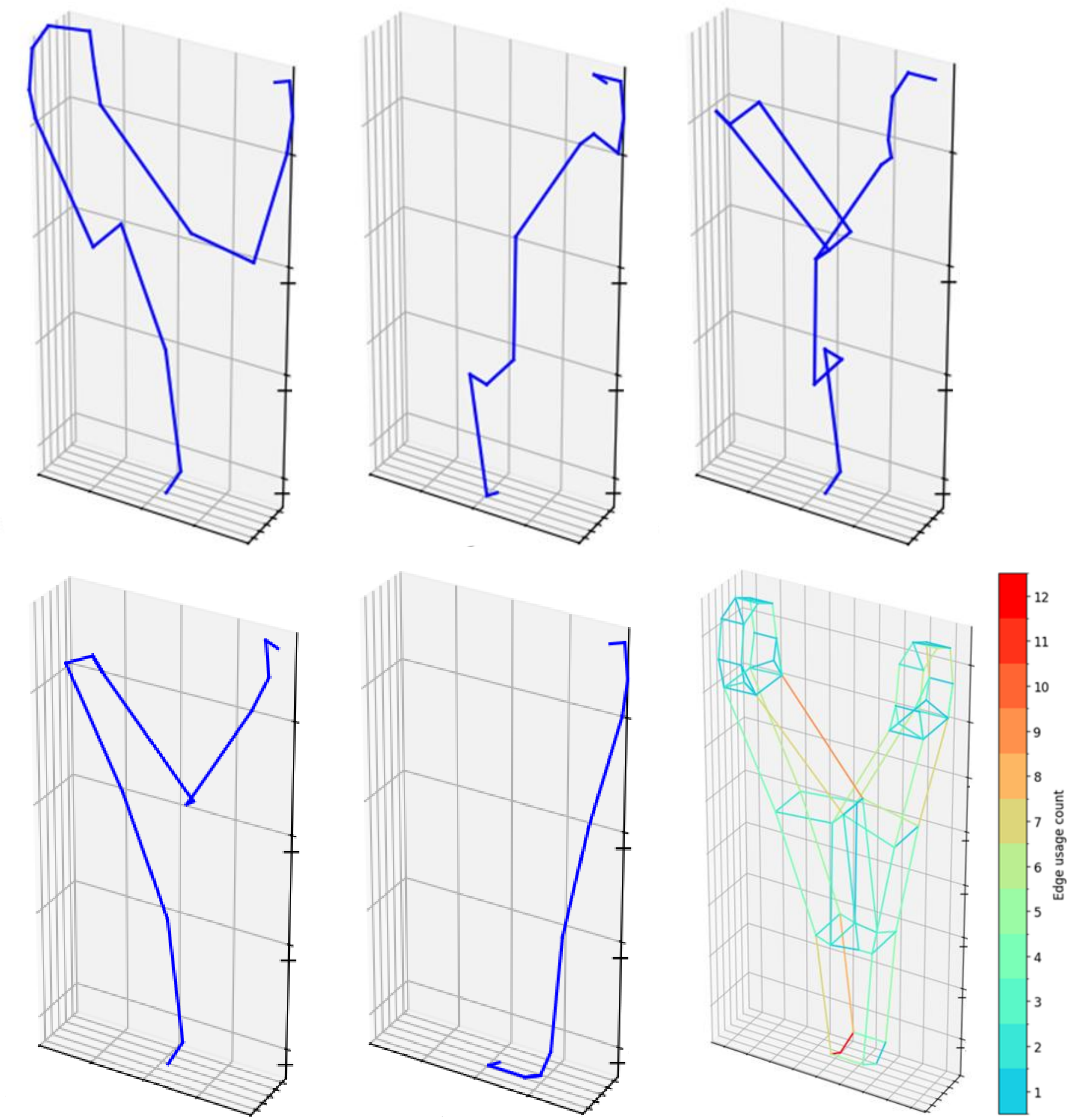

Figure 6. Five examples of interlaced yarn paths for simplified asymmetric torsion link, where the complete structure requires yarns laid along 24 paths; yarn path count over each edge, lower right.

8. Discussion, future work and conclusions

The starting point for the approach presented above was a pragmatic concept for designing 3DTO PMC parts featuring continuous yarns, as well as a manufacturing route for these parts where arrays of yarns under tension are guided and wrapped around fixed guide surfaces and interlace around each other within the boundaries of a part envelope. Actual manufacturing, which is not discussed in this paper, relies on 2 robotic manipulators exchanging a yarn carrier as the system winds yarns around obstacles in the form of supports for fixed guide surfaces guiding yarns under tension. The manufacturing system and the operations that it performs were inspired by observation of manual winding and interlacing of dry yarns into similar 3DTO structures made by operators [16]. Whilst the method described here reprises aspects present in work cited in the literature, such as the use of continuous paths of principal stresses for guiding yarn orientations as well as the practice of interlacing yarns within the part envelope to change their directions without using guides, it originates from direct observation of pragmatic manufacturing work as opposed to first principles and pure mathematical methods. Manufacturability was an ever-present concern.

Work is ongoing on both manufacturing and on the part and proceed design and optimization methodology described in this work, as discussed briefly here.

Manufacturing work conducted so far has used dry yarn almost exclusively. Introduction and consolidation of a resin remain to be addressed using either liquid resin, molten thermoplastic prepreg yarn, or thin thermosetting prepreg yarn or tape. All present challenges with regards to consolidation and external surfaces, using either mould-less processes or temporary moulds.

Yarn paths defined in step 6 are the final paths present in final parts. They do not represent paths to be programmed into robotic manipulators, especially in the case of 3DTO parts featuring direct interlacing between yarns within the volume of part envelopes, done without using guides. The final paths are created sequentially, one by one, hence intermediate paths are to be defined that will take their final configuration only after interlacing with other paths wrapped and interlaced subsequently. Equilibrium positions between interlacing yarns will depend on individual yarn tension and inter-yarn friction [16]. Predicting the outcome of interlacing arrays of parallel yarns without using guides, and controlling variability, will present challenges that were not addressed yet. Tension and friction will affect the position of interlacing points, but also the v_f and areas of yarn array cross-sections as well as their shapes, with cascading effects on resin impregnation and consolidation. Interlacing is not compulsory in specific cases but it is a desirable feature of the 3DTO PMC methodology presented here as it enables more intricate part geometries.

Step 1 of the design methodology uses isotropic material in the part envelope. An iterative sequential procedure could be used in future work, leading to orthotropic material in the envelope. Steps 2, 3, 4 and 5 are defined by clear procedures yet feature adjustable parameters. In practice, diverse utility functions are implemented for addressing practical CAD issues such as numerous vertices defined in curvatures, or to add or remove segments to parts; the methodology does enable interventions from the designer. Unequal numbers of yarns on different segments as shown in step 6 mean segments of different cross-section areas. Furthermore, areas may stay constant for a given segment, but cross-sections may change. These aspects will be addressed in future work.

9. References

[1] J. Wong, A. Altassan, and D. W. Rosen, "Additive manufacturing of fiber-reinforced polymer composites: A technical review and status of design methodologies," Composites Part B: Engineering, vol. 255, p. 110603, Apr. 2023.

[2] J. Zhu, H. Zhou, C. Wang, L. Zhou, S. Yuan, and W. Zhang, "A review of topology optimization for additive manufacturing: Status and challenges," Chinese Journal of Aeronautics, vol. 34, no. 1, pp. 91–110, Jan. 2021.

[3] M. Eckrich, P. A. Arrabiyeh, A. M. Dlugaj, and D. May, "Structural topology optimization and path planning for composites manufactured by fiber placement technologies," Composite Structures, vol. 289, p. 115488, Jun. 2022.

[4] Y. Gandhi and G. Minak, "A Review on Topology Optimization Strategies for Additively Manufactured Continuous Fiber-Reinforced Composite Structures," Applied Sciences, vol. 12, no. 21, p. 11211, Nov. 2022.

[5] X. Zhang, G. Sun, C. Wang, H. Li, and S. Zhou, "A review of structural topology optimization for fiber-reinforced composites," Composites Part B: Engineering, vol. 299, p. 112393, Jun. 2025.

[6] R. Hoglund and D. E. Smith, "Continuous Fiber Angle Topology Optimization for Polymer Fused Filament Fabrication". *Solid Freeform Fabrication 2016: Proceedings of the 26th Annual International, Solid Freeform Fabrication Symposium – An Additive Manufacturing Conference*. Austin, TX USA, pp. 1078, 2016.

[7] T. Nomura, E.M. Dede, J. Lee, S. Yamasaki, T. Matsumori, and A. Kawamoto, "General topology optimization method with continuous and discrete orientation design using isoparametric projection," Numerical Meth Engineering, vol. 101, no. 8, pp. 571–605, Feb. 2015.

[8] J. Lee, D. Kim, T. Nomura, E. M. Dede, and J. Yoo, "Topology optimization for continuous and discrete orientation design of functionally graded fiber-reinforced composite structures," Composite Structures, vol. 201, pp. 217–233, Oct. 2018.

[9] K. Zhou and X. Li, "Topology optimization of structures under multiple load cases using a fiber-reinforced composite material model," Comput Mech, vol. 38, no. 2, pp. 163–170, Jul. 2006.

[10] S. Setoodeh, M. M. Abdalla, and Z. Gürdal, "Combined topology and fiber path design of composite layers using cellular automata," Struct Multidisc Optim, vol. 30, no. 6, pp. 413–421, Dec. 2005.

[11] Y. Xu et al., "Topology optimization for additive manufacturing of CFRP structures," International Journal of Mechanical Sciences, vol. 269, p. 108967, May 2024.

[12] Z. Yang, K. Fu, Z. Zhang, J. Zhang, and Y. Li, "Topology optimization of 3D-printed continuous fiber-reinforced composites considering manufacturability," Composites Science and Technology, vol. 230, p. 109727, Nov. 2022.

[13] H. Zhang et al., "3D printing of continuous carbon fibre reinforced polymer composites with optimised structural topology and fibre orientation," Composite Structures, vol. 313, p. 116914, Jun. 2023.

[14] N. Laflamme, "On the optimization of open truss interlaced composite structures featuring continuous yarns". Master's thesis, University of Ottawa, 2025.

[15] O. Abdul-Ghani, "Topology optimization of structural continuous yarn polymer composites". Master's project report, University of Ottawa, 2026.

[16]C. Liao, "Design and optimization of open truss interlaced composite structures". MASc thesis, University of Ottawa, 2022.

[17]J. Wu, O. Sigmund, and J. P. Groen, "Topology optimization of multi-scale structures: a review," Struct Multidisc Optim, vol. 63, no. 3, pp. 1455–1480, Mar. 2021.

[18]Z. Qiu, Q. Li, Y. Luo, and S. Liu, "Concurrent topology and fiber orientation optimization method for fiber-reinforced composites based on composite additive manufacturing," Computer Methods in Applied Mechanics and Engineering, vol. 395, p. 114962, May 2022.

[19]Y. Chen and L. Ye, "Topological design for 3D-printing of carbon fibre reinforced composite structural parts," Composites Science and Technology, vol. 204, p. 108644, Mar. 2021.

[20]V. S. Papapetrou, C. Patel, and A. Y. Tamijani, "Stiffness-based optimization framework for the topology and fiber paths of continuous fiber composites," Composites Part B: Engineering, vol. 183, p. 107681, Feb. 2020.

[21]S. Nozawa and G. Serhat, "Topology and fiber path optimization of composite structures: A critical review," Materials & Design, vol. 251, p. 113699, Mar. 2025.

[22]H. Ren, D. Wang, G. Liu, D. W. Rosen, and Y. Xiong, "Concurrent optimization of structural topology and toolpath for additive manufacturing of continuous fiber-reinforced polymer composites," Computer Methods in Applied Mechanics and Engineering, vol. 430, p. 117227, Oct. 2024.

[23]H. Ye, Y. Dong, J. Yang, W. Wang, and M. Cheng, "Concurrent optimization method of principal stress orientation interpolated continuous fiber angle (PSO-CFAO) and structural topology," Composite Structures, vol. 325, p. 117572, Dec. 2023.

[24]X. Zhang, H. Ye, N. Wei, R. Tao, and Z. Luo, "Design optimization of multifunctional metamaterials with tunable thermal expansion and phononic bandgap," Materials & Design, vol. 209, p. 109990, Nov. 2021.

[25]L. Guo, Z. Meng, and X. Wang, "A new concurrent optimization method of structural topologies and continuous fiber orientations for minimum structural compliance under stress constraints," Advances in Engineering Software, vol. 195, p. 103688, Sep. 2024.

[26]H. Zhang, J. Chen, and D. Yang, "Fibre misalignment and breakage in 3D printing of continuous carbon fibre reinforced thermoplastic composites," Additive Manufacturing, vol. 38, p. 101775, Feb. 2021.

[27]H. Zhang, T. Huang, Q. Jiang, L. He, A. Bismarck, and Q. Hu, "Recent progress of 3D printed continuous fiber reinforced polymer composites based on fused deposition modeling: a review," J Mater Sci, vol. 56, no. 23, pp. 12999–13022, Aug. 2021.

[28]S. M. F. Kabir, K. Mathur, and A.-F. M. Seyam, "A critical review on 3D printed continuous fiber-reinforced composites: History, mechanism, materials and properties," Composite Structures, vol. 232, p. 111476, Jan. 2020.

[29]R. Matsuzaki et al., "Three-dimensional printing of continuous-fiber composites by in-nozzle impregnation," Sci Rep, vol. 6, no. 1, p. 23058, Mar. 2016.

[30]M. H. Ullah Khan, M. M. Islam, K. Deng, I. M. Khan, L. Liu, and K. Fu, "Additive fiber tethering for 3D architected continuous fiber composites," Composites Part A: Applied Science and Manufacturing, vol. 192, p. 108763, May 2025.

[31]M. Prado, M. Dörstelmann, T. Schwinn, A. Menges, and J. Knippers, "Core-Less Filament Winding: Robotically Fabricated Fiber Composite Building Components," in Robotic Fabrication in Architecture, Art and Design 2014, W. McGee and M. Ponce De Leon, Eds., Cham: Springer International Publishing, 2014, pp. 275–289.